Physics of semiconductor devices & renewable energies journal

Vol. 02 n. 01 (2025); ISSN 2992-040X
Journal homepage: www.psdrej.net

Kinetic Simulation of CO_2 Conversion in Dielectric Barrier Discharges

Mohamed Chenoui[1*], Hocine Tebani[1], Djilali Benyoucef[1]

[1] *Technology Department, Hassiba Benbouali UniversityLaboratoire Génie Electrique et Energies Renouvelables Chlef , Algeria*

*Corresponding author *Email: m.chenoui@univ-chlef.dz*

Abstract

In order to mitigate climate change, the use of non-thermal plasma for greenhouse gases degradation is increasingly being investigated. One of the techniques is the dissociation of carbon dioxide in cold plasma. This study focuses on modeling the dissociation of carbon dioxide in a dielectric barrier discharge plasma reactor via a one-dimensional kinetics model using COMSOL Multiphysics 5.3a package by considering 12 species and more than 55 reactions to discussed the behavior of carbon dioxide (CO_2) plasma.

Keywords: *Dielectric barrier discharge, Plasma chemical kinetic modelling, CO_2 conversion Process,*

1. Introduction

Carbon dioxide (CO_2) is a significant driver of climate change, the main cause is due to various human activities, particularly industrial manufacturing. A primary objective within the energy sector has been to transform released CO_2 into useful chemicals or fuels through chemical conversion processes [1].

DBD plasma is known for producing reactive species without high heat because the electrons within the discharge are highly energetic while the gas remains at a low temperature. The non-thermal nature enables species to be excited and ionized with minimal heating effects in the surrounding environment[2].

This makes it ideal for various industrial applications like surface treatment[3], synthesis of nanomaterials[4] ,Ozone production[5], and pollution control[6]. Furthermore, there are many studies conducted in the context of CO_2 conversion[7][8] in different parameters study effect[9][10].

In this numerical work, a model of non-thermal plasma reactor in carbon dioxide pure at air pressure employs COMSOL Multiphysics. The model allows exact regulation of operational parameters including voltage, frequency, and gas composition., enabling fine-tuning of plasma properties and reaction conditions.

The study focuses on the breakdown process and the formation of new elements during the discharge, offering a comprehensive analysis of the physical phenomena in the discharge gap.

2. Numerical model

A. Configuration and Dimensions of the Model

The model used in this work is a type of plasma discharge that occurs in a gas, where the plasma is confined in the midst of two electrodes by a dielectric substance, in a discharge gap width of 1.0 mm and a dielectric barrier thickness of 0.7 mm, having a relative permittivity equal to 9.1 [11].

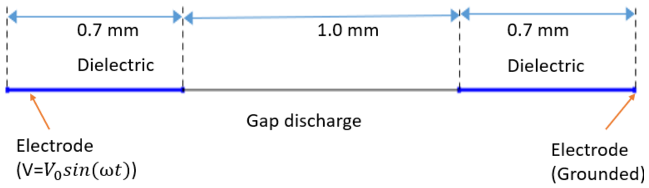

Figure 1: 1D geometry used in this work

B. Governing Equations

The description of electrons and different ions, molecules, behavior included in the model can be achieved by solving the two moments of the Boltzmann equation which describes the conservation of the momentum associated with the overall motion of the gas particles equation (1,2) and Conservation of Energy Momentum(3,4) [12].

- Electron Transport.

$$\frac{\partial \mathbf{n_e}}{\partial \mathbf{t}} + \boldsymbol{\nabla} \cdot \boldsymbol{\Gamma}_\mathbf{e} = \mathbf{R_e} \qquad (1)$$

Where n_e refers to the number of particles per unit volume and Γ_e refers to the rate of flow of particles per unit area.R_e Depends to the rate of production and loss ions due to the chemical interaction.

$$\Gamma_e = -\mu_e E n_e - \nabla(D_e n_e) \qquad (2)$$

With D_e The diffusion coefficient is related to the mobility μ_e of the positively or negatively charged atoms or molecules particles and the electrical field E in the plasma.

The energy of an electron can be determined using:

$$\frac{\partial n_\varepsilon}{\partial t} + \nabla \cdot \Gamma_\varepsilon + E \cdot \Gamma_e = R_\varepsilon \qquad (3)$$

$$\Gamma_\varepsilon = -\mu_\varepsilon E n_\varepsilon - \nabla(D_\varepsilon n_\varepsilon) \qquad (4)$$

Where ε represent the electron energy, Γ_ε represent the mean energy flux and R_ε is the electron energy either lost or gained during collisions.

Electron main energy ε computed by:

$$\varepsilon = \frac{n_\varepsilon}{n_e} \quad (5)$$

Collisional energy loss for all processes is added together to determine the electron energy loss:

$$R_\varepsilon = \sum_{i=1}^{M} x_i k_i N_n n_e \Delta\varepsilon_i \quad (6)$$

With $\Delta\varepsilon_j$ indicates the energy loss from reaction (i) the rate coefficients can be computed using cross-sectional data from LXCAT website and the next integral [7]

$$k_k = \gamma \int_0^\infty \varepsilon\sigma_k(\varepsilon) f(\varepsilon) d\varepsilon \quad (7)$$

m_e : electron mass (kg)

f : electron energy distribution function (EEDF)

q : electron charge (C)

σ_K : collision cross section (m^2) where $\gamma = \sqrt{2q/m_e}$.

- Electrostatic equations

$$-\nabla \cdot \varepsilon_0 \varepsilon_r \nabla v = \rho \quad (8)$$

ε_0 : permittivity of free space.

ε_r : permittivity of material(dielectric)

ρ : represents the charge density, which is the amount of electric charge per unit volume in a given space.

$$\rho = q\left(\sum_{k=1}^{N} Z_k n_k - n_e\right) \quad (9)$$

$Z_k n_k$: the density of (electrons / positive ions)

The driven electrode receives an electric potential:

$$V = V_0 \sin(2 * \pi * f * t) \quad (10)$$

C. Plasma Chemistry

Plasma chemistry involves different species in CO_2 model and cross section such as Elastic, Excitation, and Ionization type of reaction table (1 and 2) , three and tow-body interactions involving electrons and the heavier particles (ions and neutrals) table 3, whereas Table 4 shows surface reactions that occur when a species comes into touch with a wall.

Table 1: Species in CO2 model

Neutral	C , O, CO_2, O_2, O_3, CO
Negative ions	e−, O^-, O_2^-
Positive ions	CO_2^+ ,O^+, O_2^+

Table 2: The reactions of electron impact [13]

N	Formula	Type	ΔE (ev)
R1	$CO_2+e^- \Rightarrow CO_2+e^-$	1	0.0
R2	$CO_2+e^- \Rightarrow CO_2+e^-$	2	m/M=1.24×10^{-5}
R3	$CO_2+e^- \Rightarrow CO_2+e^-$	3	0.083
R4	$CO_2+e^- \Rightarrow CO_2+e^-$	3	0.167
R5	$CO_2+e^- \Rightarrow CO_2+e^-$	3	0.252
R6	$CO_2+e^- \Rightarrow CO_2+e^-$	3	0.291
R7	$CO_2+e^- \Rightarrow CO_2+e^-$	3	0.339
R8	$CO_2+e^- \Rightarrow CO_2+e^-$	3	0.422
R9	$CO_2+e^- \Rightarrow CO_2+e^-$	3	0.505
R10	$CO_2+e^- \Rightarrow CO_2+e^-$	3	2.5
R11	$CO_2+e^- \Rightarrow CO_2+e^-$	3	7.0
R12	$CO_2+e^- \Rightarrow CO_2+e^-$	3	10.5
R13	$CO_2+e^- \Rightarrow CO_2+e^-$	4	13.3
R14	$CO_2+e^- \Rightarrow CO_2+e^-$	4	19.1
R15	$CO_2+e^- \Rightarrow CO_2+e^-$	4	19.50
R16	$CO_2+e^- \Rightarrow CO_2+e^-$	3	1.9
R17	$CO+e^- \Rightarrow CO+e^-$	2	m/M=1.95×10^{-5}
R18	$CO+e^- \Rightarrow C+O^-$	1	0.0
R19	$CO+e^- \Rightarrow e^- + C + O$	3	11.1
R20	$CO+e^- \Rightarrow 2e^- + CO^+$	4	14
R21	$O_2+e^- \Rightarrow e^- + O_2$	2	m/M =1.7×10^{-5}
R23	$O_2+e^- \Rightarrow O + O^-$	1	0
R24	$O_2+e^- \Rightarrow e^- + 2O$	3	6.0
R25	$e^{--} + O_3 \Rightarrow e^- + O_3$	2	m/M=1.14×10^{-5}
R26	$e^- + O_3 \Rightarrow O_2^- + O$	1	0
R27	$e^- + O_3 \Rightarrow O^- + O_2$	1	0

1,2,3,4 = Attachment, Elastique, Excitation, Ionization. m/M = mass ratio.

Table 3. three-body and tow-body reactions explored in the model and their rate coefficients (m^6/s) and (m^3/s) respectively [14,15]

N	Formula	Rate coefficient
R1	$e^- + CO_2^+ \Rightarrow CO + O$	$2.0\times10^{-11}\times Te^{-0.5}\times T_g^{-1.0}$
R2	$e^- + CO_2^+ \Rightarrow C + O_2$	$3.94\times10^{-13}Te^{-0.4}$
R3	$CO_2 + O \Rightarrow CO + O_2$	$2.8\times10^{-17}exp(-26500/T_g)$
R4	$CO_2 + C \Rightarrow CO + CO$	1×10^{-21}
R5	$O_2 + CO \Rightarrow CO_2 + O$	$4.2\times10^{-18}exp(-24000/T_g)$
R6	$O_3 + CO \Rightarrow CO_2 + O_2$	4.0×10^{-31}
R7	$O^- + CO \Rightarrow CO_2 + e^-$	5.5×10^{-16}
R8	$O^- + O_2 \Rightarrow O_3 + e^-$	1.0×10^{-18}
R9	$O + O^- \Rightarrow O_2 + e$	2.3×10^{-16}
R10	$O + O_2^- \Rightarrow O_2 + O$	1.5×10^{-16}
R11	$O^- + O_3 \Rightarrow O_2 + O_2 + e^-$	3.0×10^{-16}
R12	$O_2^- + CO_2 \Rightarrow CO + O_2 + O$	6.0×10^{-13}
R13	$O + O_3 \Rightarrow O_2 + O_2$	$8.0\times10^{-18}exp(-2056/T_g)$
R14	$C + O_2 \Rightarrow CO + O$	$1.99\times10^{-16}exp(-2010/T_g)$
R15	$CO_2 +$ □ $\Rightarrow CO + O +$ □	$1.81\times10^{-16}exp(-49000/T_g)$
R16	$CO + O +$ □ $\Rightarrow CO_2 +$ □	$8.3\times10^{-46}exp(-1510/T_g)$
R17	$O_2 +$ □ $\Rightarrow O + O +$ □	$3\times10^{-12}exp(-59380/T_g)$

□ = CO2, O2 and CO, respectively.

Table 4: Surface reactions

N	Formula
R1	$CO_2^+ \Rightarrow CO_2$
R2	$O^+ \Rightarrow O$
R3	$O_2^+ \Rightarrow O_2$
R4	$O^- \Rightarrow O$
R5	$O_2^- \Rightarrow O_2$

3. Simulation results

The fluid model for DBD plasma is a numerical model that illustrates the plasma behaves in a dielectric barrier discharge (DBD) system. The densities for different species in this model are determined as a function of time and indicate the number of charged particles (ions and electrons) are present in the plasma contour.

The simulation uses a 400 K gas temperature and atmospheric pressure. A 6-Kv voltage applied with a frequency of 3 kHz.

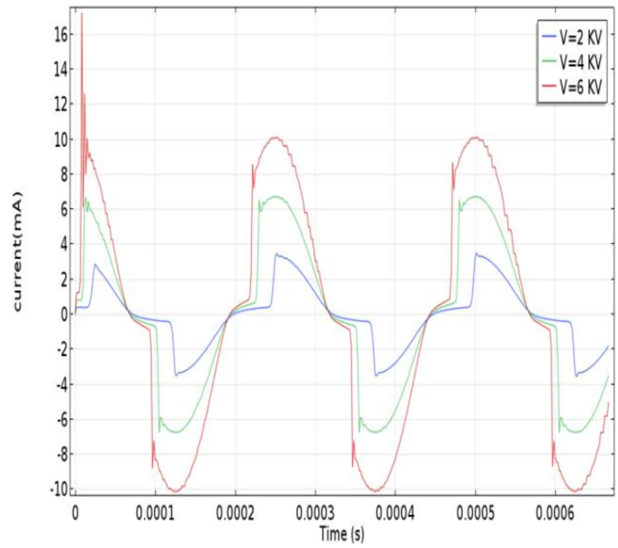

Figure 2: Discharge courant

Figure 2 show the description of the changes in electrical current over tow period of applied voltage.

Discharge current increase with voltage and there is no breakdown under 4 kV, only a streamer discharge.

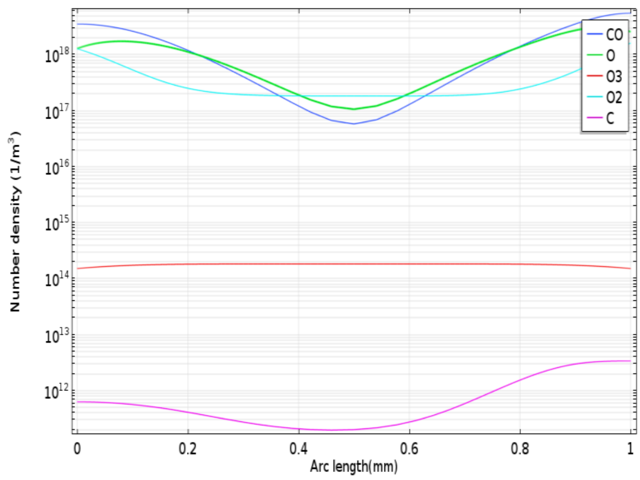

Figure 3: Different neutrals number density present in the gap

Figure 3 show primary energetic particles newly formed in the process of DBD discharge are CO,O,O_2 the density of particles O_3,C this is due to use the reduced model of carbon dioxide splitting and without mixing it with rare gases.

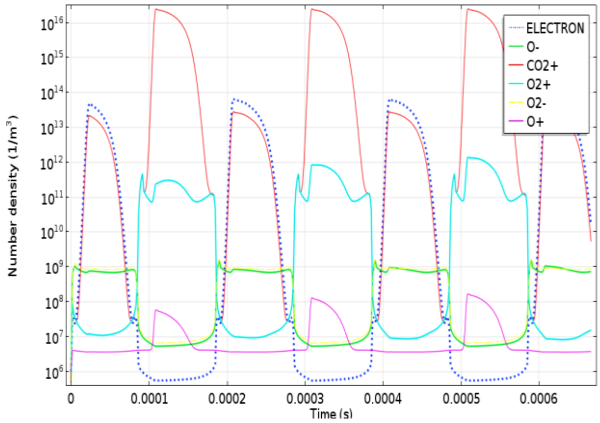

Figure 4: Temporal variation of charged species number density

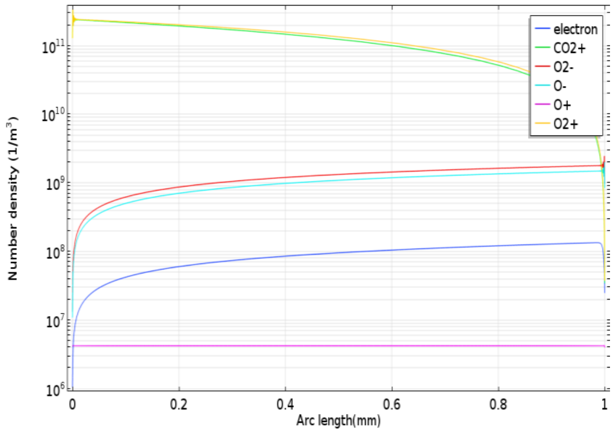

Figure 5: Different ions number density present in the gap

Figure 4 show the temporal variation of charged species number density However, at the time the voltage is applied, it generates an electric field within the gap. Electrons within this space become accelerated, potentially gaining adequate energy to start ionization. These newly formed electrons swiftly move in the direction of the grounded dielectric, accompanied by an equivalent number of ions, in Figure 5 show that O_2^- and O^- followed by CO_2^+ and O_2^+ are the most abundant ions which is consistent with the study of Rhallabi et al [11].

4. Conclusion

In this paper, we concentrate to simulate the splitting of pure carbon dioxide in non-thermal plasma reactor (DBD) at the pressure of the air via a one-dimensional model using COMSOL Multiphysics.

Our model uses a basic plasma chemistry model to highlight the physics of the carbon dioxide splitting process.to analyze 12 species behaviors in the gap, with a focus on their evolution in both space and time to gain insights into the complex physics of DBDs and capture the essential features of the discharge process. Considering all,

the existence of negative oxygen ions represents a crucial element in the functional operation of plasma actuators.

References

1. *V Marcantonio, M De Falco, E Bocci*, "Non-thermal plasma technology for CO2 conversion—an overview of the most relevant experimental results and kinetic models," Energies, vol. 15, no. 20, p. 7790, 2022.
2. Khoja, Asif Hussain, Muhammad Tahir, and Nor Aishah Saidina Amin. "Recent developments in non-thermal catalytic DBD plasma reactor for dry reforming of methane." Energy conversion and management 183 (2019): 529-560.
3. Guragain, Rajesh Prakash, et al. "Characterization of dielectric barrier discharge (DBD) produced in air at atmospheric pressure and its application in surface modification of high-density polyethylene (HDPE)." The Journal of Technological and Space Plasmas 1.1 (2020): 27-35.
4. He, Juan, et al. "Dielectric barrier discharge plasma for nanomaterials: Fabrication, modification and analytical applications." TrAC Trends in Analytical Chemistry 156 (2022): 116715.
5. China, Oi Hoong, et al. "Simulation of CO2 Decomposition in a Dielectric Barrier Discharge to Produce Ozone .
6. Heijkers, Stijn, et al. "Nanosecond pulsed discharge for CO2 conversion: kinetic modeling to elucidate the chemistry and improve the performance." The Journal of Physical Chemistry C 123.19 (2019): 12104-12116.
7. Liu, Jing-Lin, et al. "CO2 conversion, utilisation and valorisation in gliding arc plasma reactors." Journal of Physics D: Applied Physics 53.25 (2020): 253001.
8. Wang, Xu-Cheng, et al. "Comprehensive study on discharge characteristics in pulsed dielectric barrier discharges with atmospheric He and CO2." Physics of Plasmas 29.8 (2022).
9. Wang, Chao, et al. "Conversion of carbon dioxide in atmospheric pressure dielectric barrier discharges with different electrode configurations." Physica Scripta 98.8 (2023): 085605.
10. Mei, Danhua, and Xin Tu. "Conversion of CO2 in a cylindrical dielectric barrier discharge reactor: Effects of plasma processing parameters and reactor design." Journal of CO2 Utilization 19 (2017): 68-78.
11. Brehmer, F., et al. "CO and by product formation during CO2 reduction in dielectric barrier discharges." Journal of Applied Physics 116.12 (2014).
12. Zhao, Zhibo, Peng Song, and Jing Su. "Simulation study of DBD discharge characteristics and active particle-assisted methane combustion." Journal of Physics: Conference Series. Vol. 2564. No. 1. IOP Publishing, 2023.
13. LXCAT, electron scattering database, University of Toulouse,
14. France. www.lxcat.net. retrieved on January 23, 2024
15. *P Koelman*. "Chemical aspects of CO2 plasma modelling." (2019).
16. Vermeiren, Vincent. "Chemical kinetics modeling of non-equilibrium and thermal effects in vibrationally active CO2 plasmas". Diss. University of Antwerp, 2020